Experimental Study on the Optimization of Dielectric Barrier Discharge Reactor for NO_x Treatment

P. Talebizadeh, H. Rahimzadeh
Amirkabir University of Technology
Department of Mechanical engineering, Tehran, Iran

S. Javadi Anaghizi, H. Ghomi
University of Shahid Beheshti
Laser and Plasma Research Institute, Tehran, Iran

M. Babaie
University of Salford, Petroleum and Gas Engineering Division
School of Computing, Science and Engineering (CSE)
Manchester, United Kingdom

and **R.J. Brown**
Queensland University of Technology
Biofuel Engine Research Facility
Queensland, Australia

ABSTRACT

In this paper, a comprehensive study of a DBD reactor is conducted to investigate the optimum operating conditions of the reactor for NOx treatment. For each parameter, the objective is to find the maximum NOx removal efficiency with the minimum consumed power. Different effective parameters of the reactor i.e. electrode length and diameter, electrode and dielectric materials as well as parameters of power generator, i.e. voltage and frequency, are investigated. The results show that for this configuration, the electrode with 20 cm length and 10 mm diameter has the best performance. Aluminum as the inside electrode material and quartz as the dielectric material are selected. Furthermore, the optimum value for the pulse frequency is 16.6 kHz. For the mentioned optimum conditions, the NOx removal efficiency achieved is equal to almost 82% at the input power of 486 W. Furthermore, the highest achieved NOx removal is almost 92% at the input power of 864 W. The results of this paper can be used to reduce the energy consumption of NTP systems to acceptable levels.

Index Terms — **Dielectric barrier discharge reactor, non-thermal plasma optimization, NOx removal, power consumption, energy efficiency.**

1 INTRODUCTION

AMONG different air pollutants emitted by internal combustion engines, nitrogen oxides are one of the major toxic gaseous emissions. Nitrogen oxides cause a lot of deleterious effects such as respiratory and cardiovascular diseases, mortality, acid rain, ground-level ozone formation (smog), photochemical smog, global warming, nose and eye irritation, visibility impairment, the formation of toxic products and water quality deterioration [1]. Due to the mentioned adverse effects of NOx, the related legislative restrictions have become much more stringent in recent years [2]. The abbreviation NOx usually refers to the summation of NO and NO2 in emission standards. One of the main sources of NOx is motor vehicles, especially diesel engines, which emit 2-20 times more NOx than gasoline engines [3]. Up until now, several conventional technologies have been employed for NOx removal from exhaust gas such as three-way-catalyst, selective catalyst reduction (SCR), Two-Stage Fuel Injection and lime–gypsum method. However, these methods require strict operating conditions such as controlled reaction temperature and gas compositions. Furthermore, the energy efficiency and the cost of the conventional methods are still high [1, 4].

A non-thermal plasma (NTP) process, using a dielectric barrier discharge (DBD), has been introduced as a promising technology for NOx and particulate matter removal [1, 5-7]. It has great potential for emission treatment since it can operate stably at atmospheric pressure and even at low temperature [8].

Manuscript received on 19 October 2015, in final form 8 August 2016, accepted 8 August 2016.

Electric discharge plasma has been widely studied as a low cost and high energy efficiency exhaust gas treatment method in recent years [9-11]. However, more improvements are still required, especially in energy consumption, to make this technology viable in commercial use [1].

Dielectric barrier discharge reactors are used more often than other types of plasma reactors in environmental applications as a result of the easy formation of stable plasmas, homogeneous discharge, scalability, effectiveness and low operating cost [12, 13]. Due to the presence of at least one dielectric barrier between the electrodes in DBD reactors, the discharge power into the gas requires a higher voltage and therefore a higher electric field [12]. In 2001, Rajanikanth and Rout [14] investigated a dielectric packed bed reactor with and without a catalyst coating for NO removal. The studied gas consisted of cylinders containing gases of NO in N_2, N_2, CO_2 and O_2 to simulate the vehicle exhaust gas. They showed that the presence of a packed dielectric bed increases the discharge power for a given reactor size and set of operating conditions. They indicated that NO removal by NTP technology at room temperature is quite comparable with conventional catalytic converters at a high temperature of 300 °C and therefore in populated urban regions when the temperature of exhaust gas is almost 40-50 °C, the conventional catalytic converters may not be suitable at such low temperatures. In 2008, Rajanikanth and Sinha [15] studied two different types of dielectric barrier discharge electrodes, wire-cylinder reactor and pipe-cylinder reactor. They showed that for a shorter discharge gap, the discharge power consumption was higher and therefore a significant improvement in the removal efficiency of NO and NOx were achieved. They wanted to show the practical usage of this system without employing catalysts or adsorbents. In 2009, Srinivasan et al. [16] studied the effect of different voltage energizations (AC/DC/Pulse) using a DBD filled with dielectric pellets. They showed that the average electric field in the pulse energized reactor was higher than in an AC energized reactor. Furthermore, the average energy gained by the electrons under DC discharge was insufficient to generate any radicals. They also showed that using a real diesel exhaust gas increased the ability of NTP in removing NOx due to the presence of carbonaceous soot. In 2010, Matsumoto et al. [10] developed a nano-second pulse generator and indicated that a shorter pulse duration showed a great improvement in energy efficiency of NO removal. The gas cylinders of N_2 and NO in N_2 were used to simulate the exhaust gas. Moreover, they showed that increasing the length of the reactor can increase the removal efficiency of NO. In 2011 and 2012, Wang et al. [13, 17] studied a Multineedle-to-Cylinder Configuration of DBD reactor experimentally and numerically and investigated the effect of needles arrayed structure and needle arrangement on the inner electrode. They showed that by using the Multineedle-to-Cylinder system, higher performance of DBD reactor can be achieved compared to the regular DBD reactor. In 2012, Wang et al. [18] investigated different parameters of the DBD reactor, such as electrode shape and material. They showed that by using tungsten as the material of inner electrode, a higher NO removal efficiency was achieved compared to copper and stainless steel electrodes due to the higher secondary electron emission coefficient. Furthermore, changing the shape of inner electrode from rod shape to screw shape increased NO removal efficiency due to the less equivalent gap capacitance of the reactor. The specific energy density (SED) parameter is considered, in order to compare different case studies. SED is defined as the ratio of discharge power to the gas flow rate. For the same removal efficiency, it is better to have a lower specific energy density, regarding energy consumption [19]. Some researchers have also employed DBD with catalyst or adsorbent in order to increase NOx removal efficiency [20-24]. Although encouraging results have been obtained, more improvement is still required for the practical applications.

The aim of this research is to optimize the DBD reactor in terms of geometry and power generator parameters. Electrode length, diameter and material as well as dielectric material are investigated as the geometrical parameters, and the frequency and voltage of a pulse power generator are tested as the power generator parameters. The power consumption is considered as a key parameter in order to achieve the maximum NOx removal efficiency. During the experimental process, the optical emission spectroscopic method was also employed in order to provide a better understanding of the results. In this paper, different effective parameters of a DBD reactor have been examined simultaneously and the DBD reactor has been modified regarding both NOx removal and energy efficiencies. The purpose is to find the maximum NOx removal efficiency at a constant consumed power for each parameter. It should be noted that the investigations have been conducted for common geometries and materials in the literature and depending on the application and the scale of the process, the optimum values may vary and a different proposal can be recommended. Furthermore, the optimization procedure used in this paper is carried out for the first time regarding NOx removal by DBD reactors.

2 EXPERIMENTAL SETUP

The schematic of the experimental setup and the employed DBD reactor are shown in Figures. 1-a and 1-b, respectively. The setup consists of the DBD reactor, high voltage pulse power generator, gas feeding system and the measurement system [25].

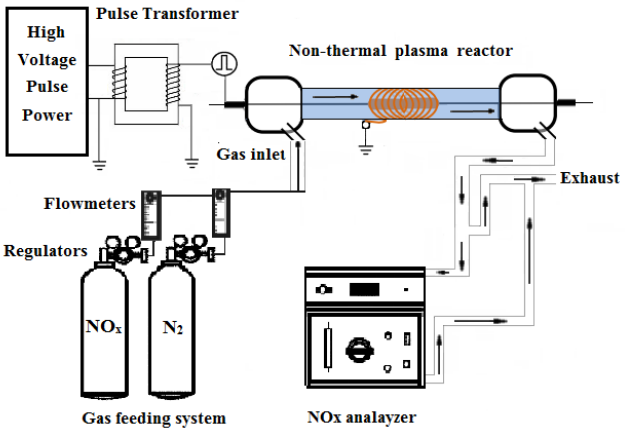

a)

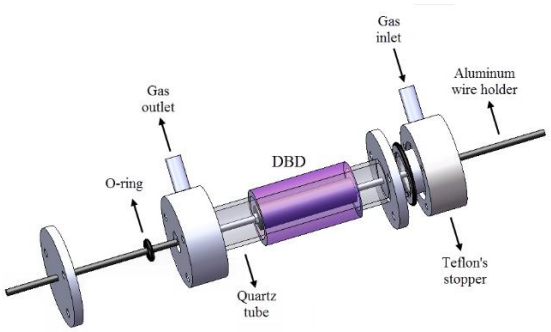

b)

Figure 1. A schematic of a) experimental setup b) DBD reactor [25].

The plasma reactor used in the present study is a DBD reactor, which is shown in Figure 1b. It is a coaxial reactor made up of two different materials of quartz glass tube (>99.9% SiO_2) and pyrex tube with the thickness of 1.5 mm and outer diameter of 15 mm. For the inner electrode, different materials i.e. aluminum, copper and steel are used to find the best operating condition. The diameters of 10, 8 and 6 mm and the lengths of 25, 20 and 15 cm are also examined in this study for the inner electrode. Note that different studied diameters of inner electrode results in different gas gaps of 2, 4 and 6 mm, respectively. An aluminum mesh is wrapped over the outer quartz glass tube, which is the grounded electrode. It should be noted that no gap should be presented between the mesh and the dielectric in order to prevent power loss [14]. It should also be noted that the materials for the electrode and dielectric and the values for the electrode diameters and lengths are chosen since they are commonly used in the literature [1]. The authors also try to examine different values for different parameters to better illustrate their effectiveness.

The experiments were performed using high-voltage DC-pulse waveform pulsed power system. The pulse power supply consists of a high voltage DC power supply, Thyratron (TGI-1-1000/25) power switches, storage capacitor, bypass inductor and stepped pulse transformer. Figure 2 shows a schematic diagram of the electric circuit. The range of output voltage of the DC power supply was 0-5 kV at maximum of 1A. The voltage was raised by pulse transformer (1:6). The DC-pulse voltage repetition rate of 10-30 kHz and peak-to-peak discharge voltage of 0-20 kV across the DBD load were generated during the experiments.

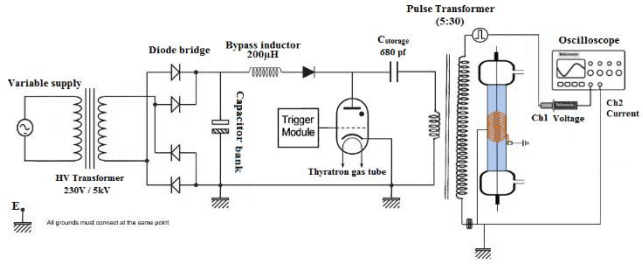

Figure 2. A schematic diagram of the electric circuit [25].

It should be noted that pulse systems provide higher performance than DC and AC systems, which is the reason for selecting pulse voltage supply in this paper. The pulsed power technology controls the duration of the discharge and protects the transition into arc discharge, providing efficient plasma chemical reaction [11, 16].

The gas system used in this study consists of two pure NOx and N_2 cylinders with the purity of industrial grade (~ 99.95%). The other gas components of NOx cylinder are N_2, H_2O, N_2O, and CO_2. The amount of each gas contained in the NOx cylinder can be found in [25]. The gas system was sealed precisely in order to prevent any gas leakage from the joints and tubes [14]. The total flow rate was 8 l/min during the experiments and the ratio of each gas was balanced while the initial concentration of NOx was adjusted to 720 ppm. All experiments were conducted at room temperature.

It should be noted that among the various types of NOx, as mentioned in the introduction, NO and NO_2 are considered toxic. Around 95% of NO_x emitted from incineration processes is NO and 5% NO_2 [1, 26]. NO is less toxic than NO_2. However, as with most radicals, NO is unstable and reacts readily with oxygen through photochemical oxidation to form NO_2 [1, 4]. Therefore, in this study, the total concentration of NO_x is considered as the polluted gas.

The concentration of NOx was measured by means of a chemiluminescence gas analyzer (AVL DI GAS 4000). It utilizes the chemiluminescence technique for analyzing the NOx concentration using a gas sample. The analyzer has a range of 0-5000 ppm and a resolution of 1 ppm of NOx. The applied voltage is measured by means of a 100-MHz digital oscilloscope (DPO 3012 TEKTRONIX) connected through a 1000:1 voltage driver (p6015 High voltage probe TEKTRONIX), and the current is measured using an AC current transformer probe (TCP202 TEKTRONIX), which includes a Rogowski coil to change the current to voltage for measuring. The pulse width is defined as full-width at half-maximum (FWHM) of the voltage, which is about 250 ns. It should be noted that the voltage and current waveforms are negative and positive, respectively. The input power was calculated by taking the product of voltage and current over one cycle of the waveforms which are obtained from a digital oscilloscope. In Figure 3, a typical waveforms of voltage and current obtained from the oscilloscope at 8.86 kV_{PP} and 13.4 kHz frequency can be seen.

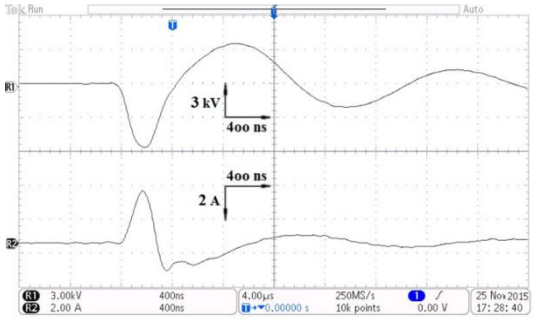

Figure 3. A typical applied voltage and current waveforms [25].

To study the effect of electrode material, the plasma

formation intensity was analyzed by an optical emission spectroscopy (OES) using a spectrometer (Ocean opticsHR2000+ES) with the accuracy of 1 nm. The range of the wavelengths considered in this study is from 200 nm to 500 nm [27]. The optic fiber of the spectrometer was placed in front of the reactor at the same position according to the reactor under the same conditions in all experiments.

It should be noted that the reactions regarding the reduction of nitrogen oxides are well established in the literature [1] and therefore not mentioned in this paper.

3 RESULTS AND DISCUSSION

As mentioned before, different geometric and power generator parameters are optimized in this paper. To provide a better understanding of different values of various studied parameters, Table 1 schematizes the studied parameters, different values considered for each parameter, the achieved optimum parameter obtained in this paper and also the related figures. It should be mentioned that all the studied materials and geometric parameters are selected since that they have been used more in the literature.

Note that for some parameters such as pulse frequency and electrode length, in the studied range, the results for different values of each parameter are close to each other and therefore an optimum parameter interval can be given; however, the best cases among the examined values of each parameter is given in Table 1.

Table 1. Range of parameters investigated and summary of optimum values in this study.

Parameter	Studied range	Optimum value	Related Figure
Electrode Material	Al, Cu, St	Al	4-5-6
Dielectric Material	quartz, pyrex	quartz	7-8-9
Electrode Length	15, 20, 25 cm	20 cm	10-11
Electrode Diameter	6, 8, 10 mm	10 mm	12-13-14
Pulse voltage	7.1, 8.7 and 9.9 kV_{PP}	9.9 kV_{PP}	15-16
Pulse frequency	13.4, 16.6, 21.9, 27.2 kHz	16.6 kHz	17-18

Note that for the geometric parameters, all the experiments were conducted at three different frequencies of 16.6, 21.9 and 27.2 kHz and different applied voltages of 7.1, 8.7 and 9.9 kV_{PP}. In Table 1, V_{PP} is the peak-to-peak discharge voltage across the DBD load.

In the following sections, the effects of different parameters listed in Table 1 are discussed in detail.

3.1. EFFECT OF ELECTRODE MATERIAL

To study the effect of electrode material, three different materials were tested including aluminum, copper and steel. Figure 4 presents the effect of electrode material on NOx removal efficiency for various pulse frequencies at 8.7 kV_{PP}. It should be noted that NOx removal efficiency is calculated from the following equation:

$$NOx_R = \frac{NOx_i - NOx_f}{NOx_i} \times 100 \quad (1)$$

where NOx_i and NOx_f are initial (before treatment) and the final (after treatment) concentrations of NOx in the gas mixture, respectively.

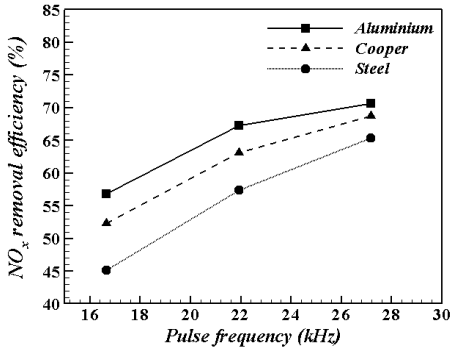

Figure 4. Effect of electrode material on NOx removal efficiency at 8.7 kV_{PP} and different pulse frequencies.

As presented in Figure 6, aluminum shows a better performance than copper and steel for NOx reduction. The reason is the secondary electron emission coefficient, γ, which represents the electron emission efficiency from the cathode due to positive ion bombardment [28]. Increasing γ means more electron and ion production in the plasma state. Therefore, the mean kinetic energy of the ions for bombarding the cathode increases and higher discharge power can be achieved [28]. Since the secondary electron emission coefficients for aluminum, copper and steel are 1.5, 1.29 and 1.24, respectively; aluminum as the inside electrode shows a better performance than the other two materials. Note that tungsten is also used in the literature as the inner electrode material; however, since the secondary electron emission coefficient of tungsten is less than aluminum, it is not studied in this paper. Another important issue is that in the plasma state, the aluminum should be assumed to be strongly oxidized which increases the secondary electron emission coefficient of the inner electrode and therefore more NOx can be removed from the exhaust gas.

This can also be explained regarding the breakdown voltage [29]. The breakdown voltage is a function of the secondary electron emission coefficient. The breakdown voltage decreases by increasing the secondary electron emission coefficient. Therefore, a smaller breakdown voltage is required for a material with higher secondary electron emission coefficient for introducing the plasma. Higher NOx removal can be achieved with a smaller breakdown voltage since the reduction reactions of NOx can be happened earlier at the plasma state. Furthermore, a higher secondary electron emission coefficient leads to a higher number of generated electrons which strengthen the plasma chemical reactions and more NOx are removed from the exhaust gas. It is also notable that aluminum is cheaper than copper and steel, which is another advantage for aluminum [30].

It should be noted that, as shown in Figure 4, the difference of NO_x removal efficiency is the same order or even larger between copper and steel than that of aluminum. The reason may be due to the fact that for higher removal efficiencies, the effect of two quantities is less established than that of lower removal efficiencies. For example, as shown in Figure 4, the difference between the NOx removal efficiency of aluminum and copper is higher at the beginning of the diagram and reaches to a smaller value by increasing the pulse frequency. Therefore, the reason for the higher difference of NOx removal efficiency between aluminum and copper than that of copper and steel can be due to the mentioned reason. Furthermore, a lot of parameters can be effective when studying an especial quantity in the plasma environment and considering all of them together cannot be possible.

For better understanding of the effect of electrode material, the optical emission spectrum of the NOx plasma discharge for different electrode materials was measured. The emission spectrum of the plasma discharge in NOx showed peaks of N_2 second positive band system and NOγ band system [31, 32]. These band systems refer to the occurrence of a change in the molecular excitation level of each element in the emission spectrum of an electric discharge [33]. Table 1 lists the detected peaks of the wavelengths for N_2 second positive band systems and NOγ band system. As listed, the second positive band of molecular nitrogen is the result of the spontaneous de-excitation of the molecule from the $C^3\Pi$ to the $B^3\Pi$ electronic state [33]. $C^3\Pi$ and $B^3\Pi$ electronic states are lying at 11.0 and 7.4 eV above the ground electronic state, respectively [34]. The electron mean energy in non-thermal plasma depends on the experimental conditions such as gas composition and applied voltage [35].

Table 2. The detected peaks of the wavelengths for N_2 second positive band systems and NOγ band system.

Species (system)	Transitions	Peak positions (nm)
N_2 second positive band	$C^3\Pi \rightarrow B^3\Pi$	315; 337.1; 357.7; 380.5
NOγ band	$A^2\sum^+ \rightarrow X^2\sum^+$	237; 247.9; 259.6; 271.5

According to the N_2 second positive band system, excitation of nitrogen molecules in the ground state by direct electron impact is performed as follows [27, 36]:

$$e + N_2(X^1\sum_g^+)_{v=0} \rightarrow N_2(C^3\pi_u)_{v'=0} + e(\Delta E = 11eV) \quad (2)$$

and then, spontaneous radiation of formed excited state of nitrogen makes $N_2(B^3\pi_g)$ as follows [27, 36]:

$$N_2(C^3\pi_u)_{v'=0} \rightarrow N_2(B^3\pi_g)_{v''=0} + h\nu \quad (3)$$

The NOγ band is excited by the collision of N_2 metastable states as follows [31, 37]:

$$N_2(A) + NO(X) \rightarrow N_2(X) + NO(A) \quad (4)$$

$$NO(A) \rightarrow NO(X) + h\nu(NO_\gamma\ band) \quad (5)$$

Figure 5 represents emission spectrum of the plasma discharge in NOx for different materials of inner electrode inside electrode materials. The spectrum was obtained at 8.7 kV_{PP} and 19.2 kHz pulse frequency. As shown, the intensities of peaks for N_2 second positive band system and NOγ band system for aluminum as the material of inner electrode are higher than those measured for copper and steel. The highest intensity of N_2 second positive band and NOγ band occur at the wavelengths of 336.7 nm and 247.8 nm, respectively.

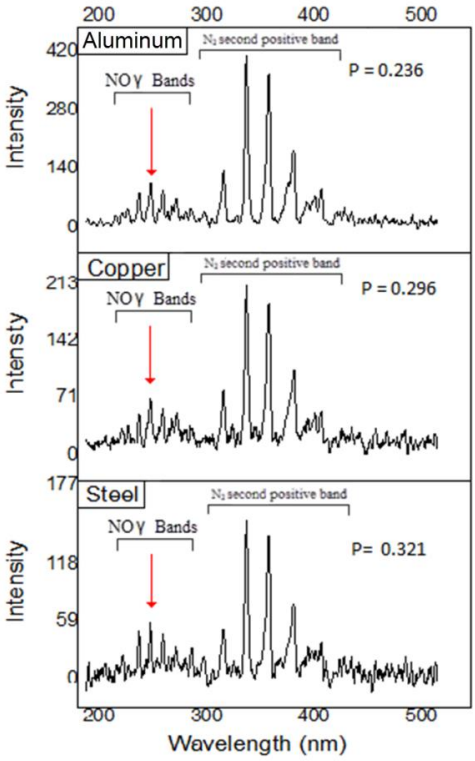

Figure 5. The emission bands of N_2 second positive band and NOγ band for the different studied materials in 8.7 kV_{PP} and 19.23 kHz pulse frequency.

The relation between the captured intensities of N_2 second positive band and NOγ band is the proof for removing higher NOx concentration. The higher ratio of N_2 second positive band to the NOγ band means higher production of N_2 related to NO_x and therefore, less NOx exits from the exhaust gas. To provide a criterion for the ratio of N_2 second positive band to the NOγ band, a parameter is defined in this study, which can be calculated by the following equation:

$$P = \frac{Highest\ Intensity\ of\ NO_\gamma\ bands}{Highest\ Intensity\ of\ N_2\ second\ positive\ bands} \quad (6)$$

P is defined as the ratio of the highest intensity of the gas pollutant atoms (NOγ) to the highest intensity of nitrogen atoms at the wavelength peaks. When the value of P increases, it means the ratio of NOγ bands to the N_2 second positive bands increases and therefore, higher NOx concentration is existed in the plasma state [37]. By calibration of captured spectra with the highest intensity of nitrogen atoms (setting the initial condition of the system equal to the N_2

highest intensity), the value of P will be equal to the highest intensity of NOγ bands. According to Figure 5, the P values for aluminum, copper and steel is 0.236, 0.296 and 0.321, respectively. Therefore, aluminum is better than the other two studied materials in terms of NOx removal efficiency.

Figure 6 shows the variation of NOx removal as a function of both input power and specific input energy for the studied materials. The specific input energy (SIE) is an important quantity in the study of non-thermal plasma which is given as:

$$SIE = \frac{E \times 60\,[s/\min] \times 22.4\,[l/mole]}{G} \qquad (J/mole) \qquad (7)$$

where E (W) is the input power to the reactor and G $(l/\min)$ is the gas flow rate. It means the amount of input energy that applied to 1 mole of NO_x. Note that 1 mole NO_x is equal to $30\,(g)$ NO and $46\,(g)$ NO_2 which is equivalent to $22.4\,(l)$ at atmospheric pressure and $273\,(K)$. By using the mentioned information, the data in Figure 6 can be easily converted to g/kWh which is also a usual quantity regarding non-thermal plasma investigations.

As shown in the figure, aluminum has the most NOx removal efficiency compared to copper and steel for the same input power especially at the removal efficiency of more than 80%. As mentioned before, the reason is the higher secondary electron emission coefficient of aluminum. Since aluminum has a higher γ compared to copper and steel at the same input power, the reactor with aluminum as the inside electrode material has less breakdown voltage and therefore, more NOx is reduced. Note that for different electrode materials, the difference between NOx removal efficiency is not significantly high; however, aluminum has the best performance among the other considered electrodes.

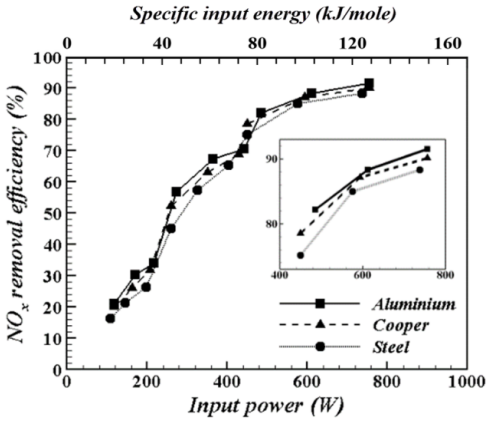

Figure 6. Effect of electrode material on NOx removal efficiency for different input powers.

The result from this section of the experiment shows that aluminum is the best material for the inside electrode among the studied materials regarding both NOx removal efficiency and power consumption.

3.2 EFFECT OF DIELECTRIC MATERIAL

To study the dielectric material, two different materials are examined: quartz and pyrex. Figure 7 presents the effect of dialectic material on NOx removal efficiency for various pulse frequencies at the applied voltages of 7.1 and 9.9 kV.

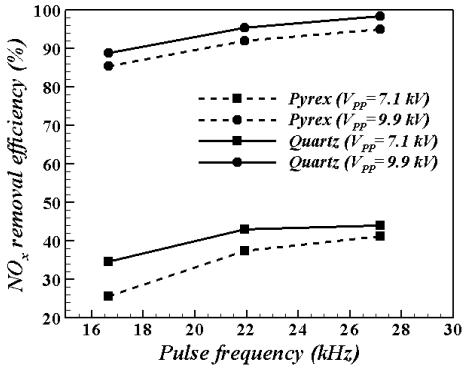

Figure 7. Effect of dielectric material on NOx removal efficiency for different pulse frequencies and voltages.

As shown, quartz as the dielectric material shows a better performance than pyrex for NOx removal. The reason can be explained in conjunction with the electric permittivity coefficient. Selecting a material with a higher electric permittivity coefficient results in a higher discharge power and therefore the gas breakdown will happen at lower applied voltage and more NOx can be removed during the plasma treatment. The electric field at radius r in the discharge gap is defined as [18]:

$$E_g(r) = \frac{1}{\ln\left(\frac{r_{d2}}{r_c}\right) - \left(\frac{\varepsilon_d - \varepsilon_g}{\varepsilon_d} \times \frac{l_d}{r_{d1}}\right)} \times \frac{V}{l_g} \qquad (8)$$

where ε_d and ε_g are dielectric constant or electric permittivity coefficient of the dielectric barrier layer and gas, r_c is the radius of the electrode, r_{d1} and r_{d2} are the inner and outer radius of the dielectric barrier (tube) layer, l_d is equal to the dielectric thickness ($l_d = r_{d2} - r_{d1}$), l_g is equal to the discharge gap ($l_g = r_{d1} - r_c$) and V is the voltage.

The calculated electric field before the breakdown in the discharge gap versus the distance from the inner electrode for quartz and pyrex at 8.7 kV_{PP} is shown is Figure 8. The gas specifications are assumed to be similar to air ($\varepsilon_g = 1$) and the electric permittivity coefficient for quartz and pyrex is 5 and 4.1, respectively. The electric field obtained for the reactor with quartz dielectric is stronger than the reactor with pyrex. In other words, at the same distance from the inner electrode, the intensity of the electric field for the reactor with quartz dielectric is higher than the one with pyrex dielectric.

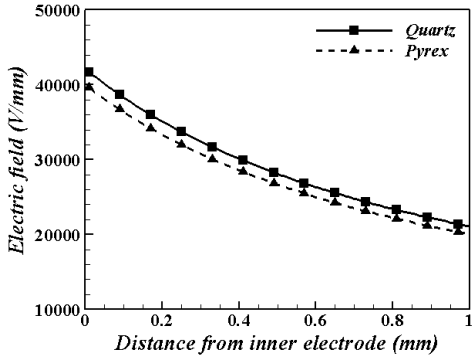

Figure 8. The effect of dielectric material on the electric field as a function of distance from inner electrode.

Figure 9 compares NOx removal efficiency for the reactors with quartz and pyrex dielectrics. As shown, for all input powers, NOx removal efficiency for quartz dielectric is higher than pyrex dielectric due to the occurrence of a higher electric field for all applied voltages and frequencies. It can also be explained with respect to the electrical capacitance. Higher electrical capacitance can be achieved by higher electric permittivity and stronger plasma can be generated by a dielectric with higher electrical capacitance due to the reactor impedance [18, 38].

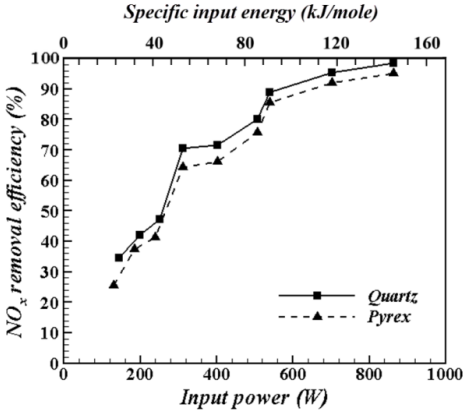

Figure 9. Effect of dielectric material on NOx removal efficiency for various input powers.

The result from this section of the experiment shows that quartz as the dielectric material has better performance than pyrex in terms of both power consumption and NOx removal efficiency.

3.3 EFFECT OF ELECTRODE LENGTH

To study the effect of electrode length, three different lengths are considered for the DBD reactor: 15, 20 and 25 cm. Figure 10 illustrates the effect of electrode length on NOx removal efficiency for various pulse frequencies at 7.1 kV_{PP}. Note that in this experiment, aluminum and quartz are selected for the inside electrode and dielectric material, because of their better performance, as confirmed in the previous section of this paper.

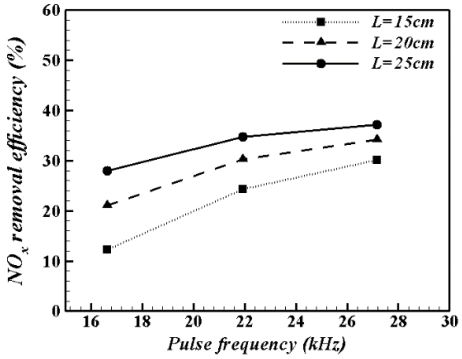

Figure 10. Effect of electrode length on NOx removal efficiency at 7.1 kV_{PP} and different pulse frequencies.

As shown, NOx removal efficiency is increased by increasing the electrode length. The reason is as a result of increasing the pulse discharge current. The current increases by changing discharge impedance mismatching with increasing the reactor length due to the raise of the produced streamer channels. Consequently, with approximately constant applied voltage for different electrode lengths, higher discharge power is achieved by using a longer electrode and therefore, more NOx can be removed from the exhaust gas [39]. Furthermore, the increase of electrode length increases the gas residence time. Therefore, the gas is under the plasma state for more time to the plasma and more NOx can be removed from the exhaust gas [25, 40]. However, increasing the NOx removal efficiency is due to the increase in the electrical energy consumption. Figure 11 shows the variation of NOx removal efficiency at different input powers and different SIE for various electrode lengths. As shown, at the high range of NOx removal efficiency (more than 75%), the NOx removal efficiency for 20 cm electrode length is higher than 15 and 25 cm electrode length. It is concluded that according to the consumed power, the electrode with the length of 20 cm is more applicable than the other two electrode lengths. It should be noted that the difference between NOx removal efficiency for the studied electrode length is not significant; however, the electrode with the length of 20 cm has the best performance among the others.

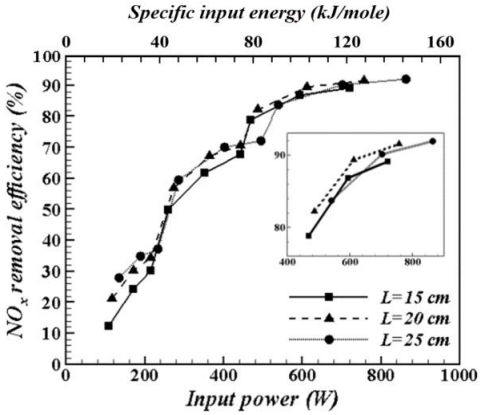

Figure 11. Effect of electrode length on NOx removal efficiency for different input powers.

The result from this section of the experiment shows that by selecting the length of electrode equal to 20 cm, the optimum performance of the reactor can be achieved among the other studied electrode lengths.

3.4 EFFECT OF ELECTRODE DIAMETER

In this section, the experiments have been carried out by using the electrode with the length of 20 cm with different diameters. The effect of corona electrode diameter on NOx removal efficiency for various pulse frequencies at 8.7 kV_{PP} is shown in Figure 12.

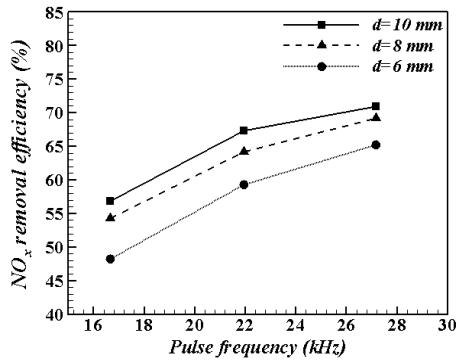

Figure 12. Effect of electrode diameter on NOx removal efficiency at 8.7 kV_{PP} and different pulse frequencies.

As shown, the electrode with the largest diameter shows the highest NOx removal efficiency. The calculated electric field, as a function of distance from inner electrode for three different electrode diameters before the start of breakdown, is shown in Figure 13. The gas specifications are assumed to be the same as air ($\varepsilon_g = 1$) and the dielectric constant of the quartz tube is 5. As shown, the electrode with 10 mm diameter has the strongest electric field among the studied electrodes. In other words, at the same distance from the inner electrode, the intensity of electric field for the electrode with 10mm diameter is higher than the other electrodes. Therefore, this electrode has higher NOx removal efficiency than the others.

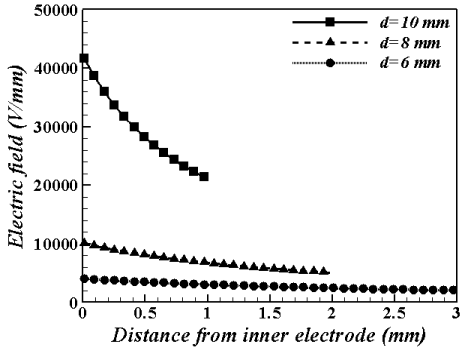

Figure 13. The effect of electrode diameter on the electric field as a function of distance from inner electrode at 8.7 kV_{PP}.

Figure 14 presents the variation of NOx removal efficiency as a function of both input power and SIE for different electrode diameters. As shown, the NOx removal efficiency is higher for the electrode with diameter of 10 mm. The reason is the higher input power requirement to obtain the same NOx removal efficiency for the smaller electrode diameter.

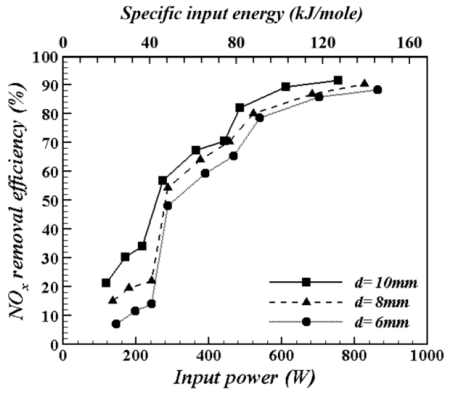

Figure 14. Effect of electrode diameter on NOx removal efficiency for different input powers

The result from this section of the experiment shows that the electrode with 10 mm diameter has the best performance among the other electrodes in terms of both NOx removal efficiency and power consumption.

3.5 EFFECT OF APPLIED VOLTAGE AND PULSE FREQUENCY

Figure 15 displays the variation of NOx removal efficiency with different pulse frequency and different voltage levels for the optimized reactor parameters i.e. 10 mm electrode diameter, 20 cm electrode length, quartz as a dielectric material and aluminum as the electrode material. As expected, the NOx removal efficiency is increased by increasing the applied voltage and pulse frequency.

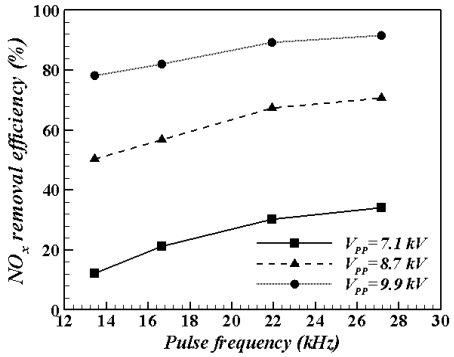

Figure 15. The variation of NOx removal efficiency with various pulse frequency for different applied voltage.

Increasing the applied voltage results in an increase in the electric field, which means that a stronger electric field is generated inside the reactor. Furthermore, regarding Eq. 15, the electric field before the breakdown in the discharge gap has a direct relation to the applied voltage. Therefore, a higher electric field is achieved by increasing the applied voltage and accordingly higher NOx removal efficiency is achieved by V_{PP}=9.9 kV.

Increasing the pulse frequency results in a higher input power [41]. Table 3 presents the produced input power as well as specific input energy for different pulse frequency at 8.7 kV_{PP}. As shown, the input power increases from 208 W to 442 W when the pulse frequency is increased from 13.4 kHz to 27.2 kHz, which results in a higher NOx removal from the gas. Furthermore, by increasing the pulse frequency, the charge and discharge rate of the storage capacitor in the pulse power system is increased and consequently, the effective collisions of electrons, ions, atoms and molecules will increase. Therefore, more NOx removal can be achieved.

Table 3. Input power for different pulse frequency at V_{PP}=8.7 kV.

Unit Frequency	Input power	Specific input energy
13.4 kHz	208 W	34.9 kJ/mole
16.6 kHz	273 W	45.9 kJ/mole
21.9 kHz	364 W	61.2 kJ/mole
27.2 kHz	442 W	74.3 kJ/mol

Figure 16 shows the variation of NOx removal efficiency as a function of both input power and SIE for various pulse frequencies. The power is almost proportional to the pulse frequency. Therefore, the maximum power is limited to the value of pulse frequency [42]. As shown in the figure, for the same input power, the NOx removal efficiency is almost higher at the lower frequencies [41, 43]. However, at the very low frequencies such as 13.4 kHz, high input power and, as a result, high removal efficiency cannot be achieved at the studied range of applied voltages. In other words, obtaining a high range of input powers is restricted by the highest applied voltage of the system. Therefore, in this paper, the frequency of 16.6 kHz is found to be the optimum frequency. It can be concluded that increasing the frequency beyond a certain limit cannot improve the NOx removal efficiency.

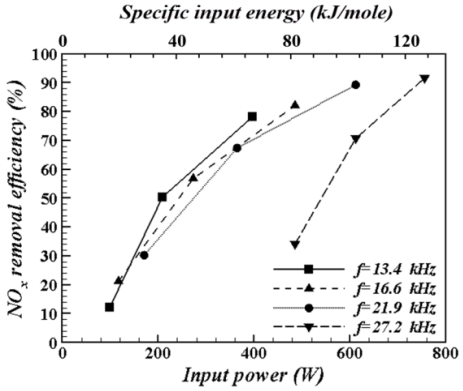

Figure 16. Effect of pulse frequency on NOx removal efficiency for different input powers.

It is shown that for a certain input power, higher NOx removal efficiencies may be obtained at lower frequencies. However, higher input power can be achieved at higher frequencies [42, 44].

Figure 17 shows the variation of NOx removal efficiency for different input powers and different SIE at various applied voltages. As shown in this figure, by increasing the applied voltage, the input power and also NOx removal efficiency increase.

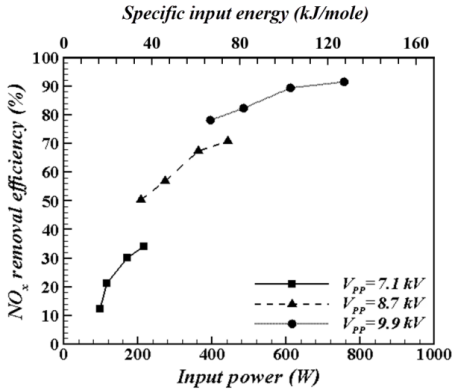

Figure 17. Effect of applied voltage on NOx removal efficiency for different input powers.

Against the pulse frequency effect, increasing the applied voltage is always effective for removing NOx from the exhaust gas.

Figures. 18-a and 18-b display the waveforms of discharge voltage and current for the frequency of 16.6 kHz and different V_{PP}, respectively. The discharge voltage is increased by increasing the applied voltage and, as shown in Figure 18b, the discharge current is increased as well. Therefore, the discharge power as a function of discharge voltage and current increases and more NOx removal can be achieved.

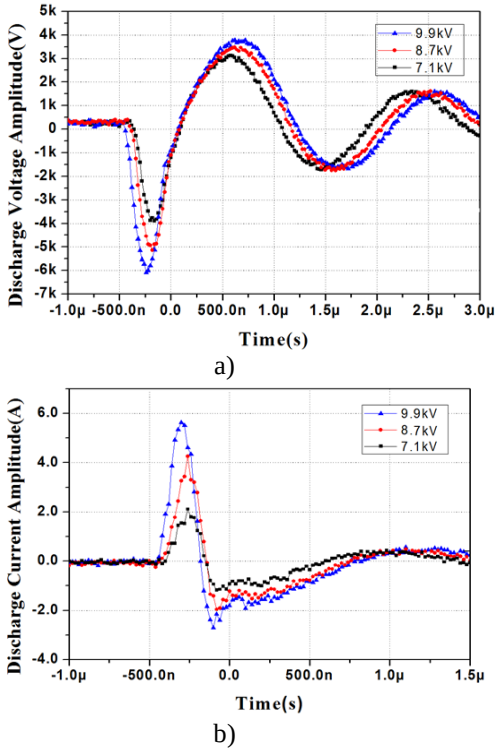

Figure 18. a) The discharge voltage waveforms b) The discharge current waveform for different applied voltages

4 CONCLUSION

In this paper, an experimental optimization is performed in order to find the best values for the effective parameters of dielectric barrier discharge reactor, regarding both NOx removal efficiency and power consumption. The results showed that aluminum and quartz are the best materials for the inner electrode and dielectric material, respectively. Furthermore, the electrode with the diameter of 10 mm and length of 20 cm has the best performance. Increasing the voltage is always effective for both NOx removal efficiency and power consumption. However, the frequency of 16.6 kHz shows better performance than the other studied frequencies. For the optimum cases, the achieved NOx removal efficiency is equal to almost 82% at the input power of 486 W. In general, the highest achieved NOx removal is almost 92% at the input power of 864 W. This study sheds a light on the approach towards the possibility of an optimization process and the results of this paper could be considered as an effective method for commercialization of this technology in the future. Furthermore, the optimization procedure used in this paper is carried out for the first time regarding NOx treatment by NTP DBD reactors.

REFERENCES

[1] P. Talebizadeh, M. Babaie, R. Brown, H. Rahimzadeh, Z. Ristovski, and M. Arai, "The role of non-thermal plasma technique in NOx treatment: A review," Renewable Sustainable Energy Reviews, Vol. 40, pp. 886-901, 2014.

[2] T. Nüesch, A. Cerofolini, G. Mancini, N. Cavina, C. Onder, and L. Guzzella, "Equivalent Consumption Minimization Strategy for the Control of Real Driving NOx Emissions of a Diesel Hybrid Electric Vehicle," Energies, Vol. 7, pp. 3148-3178, 2014.

[3] J. Riess, "NOx : how nitrogen oxides affect the way we live and breathe," U.S. Environmental Protection Agency, Office of Air Quality Planning and Standards, 1998.

[4] K. Skalska, J. S. Miller, and S. Ledakowicz, "Trends in NOx abatement: A review," Science Total Environment, Vol. 408, pp. 3976-3989, 2010.

[5] J.-S. Chang, "Next generation integrated electrostatic gas cleaning systems," J. Electrostatics, Vol. 57, pp. 273-291, 2003.

[6] J. O. Chae, "Non-thermal plasma for diesel exhaust treatment," J. Electrostatics, Vol. 57, pp. 251-262, 2003.

[7] M. Babaie, P. Davari, P. Talebizadeh, F. Zare, H. Rahimzadeh, Z. Ristovski, R. Brown, "Performance evaluation of non-thermal plasma on particulate matter, ozone and CO2 correlation for diesel exhaust emission reduction," Chem. Eng. J., Vol. 276, pp. 240-248, 2015.

[8] B. Eliasson and U. Kogelschatz, "Nonequilibrium volume plasma chemical processing," IEEE Trans. Plasma Sci., Vol. 19, pp. 1063-1077, 1991.

[9] R. Hackam and H. Aklyama, "Air pollution control by electrical discharges," IEEE Trans. Dielectr. Electr. Insul., Vol. 7, pp. 654-683, 2000.

[10] T. Matsumoto, D. Wang, T. Namihira, and H. Akiyama, "Energy Efficiency Improvement of Nitric Oxide Treatment Using Nanosecond Pulsed Discharge," IEEE Trans. Plasma Sci., Vol. 38, pp. 2639-2643, 2010.

[11] B. M. Penetrante, "Pollution control applications of pulsed power technology," IEEE 9th Pulsed Power Conf., pp. 1-5, 1993.

[12] U. Kogelschatz, "Dielectric-barrier Discharges: Their History, Discharge Physics, and Industrial Applications," Plasma Chem. Plasma Processing, Vol. 23, pp. 1-46, 2003.

[13] X. Wang, Q. Yang, C. Yao, X. Zhang, and C. Sun, "Dielectric Barrier Discharge Characteristics of Multineedle-to-Cylinder Configuration," Energies, Vol. 4, pp. 2133-2150, 2011.

[14] B. S. Rajanikanth and S. Rout, "Studies on nitric oxide removal in simulated gas compositions under plasma-dielectric/catalytic discharges," Fuel Processing Technology, Vol. 74, pp. 177-195, 2001.

[15] B. S. Rajanikanth and D. Sinha, "Achieving better NO_x removal in discharge plasma reactor by field enhancement," Plasma Sci. Technology, Vol. 10, pp. 198-202, 2008.

[16] A. D. Srinivasan, B. S. Rajanikanth, and S. Mahapatro, "Corona Treatment for NO_x Reduction from Stationary Diesel Engine Exhaust Impact of Nature of Energization and Exhaust Composition," Electrostatics joint conf., pp. 44150, 2009.

[17] X. Wang, C. Yao, C. Sun, Q. Yang, and X. Zhang, "Numerical Modelling of Mutual Effect among Nearby Needles in a Multi-Needle Configuration of an Atmospheric Air Dielectric Barrier Discharge," Energies, Vol. 5, pp. 1433-1454, 2012.

[18] T. Wang, B.-M. Sun, H.-P. Xiao, J.-y. Zeng, E.-p. Duan, J. Xin, *et al.*, "Effect of Reactor Structure in DBD for Nonthermal Plasma Processing of NO in N2 at Ambient Temperature," Plasma Chem. Plasma Processing, pp. 1-13, 2012.

[19] J. Hoard, P. Laing, M. Balmer, and R. Tonkyn, "Comparison of Plasma-Catalyst and Lean NOx Catalyst for Diesel NOx Reduction," SAE Technical paper,Vol. 01, pp. 2895, 2000.

[20] T. Yamamoto, M. Okubo, K. Hayakawa, and K. Kitaura, "Towards ideal NO x control technology using a plasma-chemical hybrid process," IEEE Trans. Industry Applications, Vol. 37, pp. 1492-1498, 2001.

[21] M. Okubo, M. Inoue, T. Kuroki, and T. Yamamoto, "NOx reduction aftertreatment system using nitrogen nonthermal plasma desorption," IEEE Trans. Industry Appl., Vol. 41, pp. 891-899, 2005.

[22] S. Mohapatro and B. S. Rajanikanth, "Cascaded cross flow DBD-adsorbent technique for NOx abatement in diesel engine exhaust," IEEE Trans. Dielectr. Electr. Insul., Vol. 17, pp. 1543-1550, 2010.

[23] T. Yamamoto, S. Asada, T. Iida, and Y. Ehara, "Novel NOx and VOC treatment using concentration and plasma decomposition," IEEE Trans. Industry Appl., Vol. 47, pp. 2235-2240, 2011.

[24] A. K. Srivastava and G. Prasad, "Characteristics of parallel-plate and planar-surface dielectric barrier discharge at atmospheric pressure," J. Electrostatics, Vol. 72, pp. 140-146, 2014.

[25] S. J. Anaghizi, P. Talebizadeh, H. Rahimzadeh, and H. Ghomi, "The Configuration Effects of Electrode on the Performance of Dielectric Barrier Discharge Reactor for NOx Removal," IEEE Trans. Plasma Sci., Vol. 43, pp. 1944-1953, 2015.

[26] M. A. Gómez-García, V. Pitchon, and A. Kiennemann, "Pollution by nitrogen oxides: an approach to NOx abatement by using sorbing catalytic materials," Environment Int'l., Vol. 31, pp. 445-467, 2005.

[27] M. Blajan, S. Muramatsu, T. Ishii, H. Mimura, and K. Shimizu, "Emission Spectroscopy of Microplasma Driven by a Pulsed Power Supply," J. Inst. Electrostat. Jpn., Vol. 34, pp. 99-104, 2010.

[28] X. Xu and T. C. Zhu, *Gas Discharge Physics*, Shanghai: Fudan University Press, 1996.

[29] R. V. Latham, *High Voltage Vacuum Insulation: Basic Concepts and Technological Practice*: Elsevier Science, 1995.

[30] V. Baglin, J. Bojko, O. Grobner, B. Henrist, N. Hilleret, C. Scheuerlein, M. Taborelli,"The secondary electron yield of technical materials and its variation with surface treatments," European Particle Accelerator Conf., Austria, pp. 217-221, 2000.

[31] M. Blajan, T. Ishii, H. Mimura, and K. Shimizu, "Emission spectrometry of microplasma for NOx removal process," 19th Int'l Symp. on Plasma Chemistry, pp. 398, 2009.

[32] F. Liu, W. Wang, S. Wang, W. Zheng, and Y. Wang, "Diagnosis of OH radical by optical emission spectroscopy in a wire-plate bi-directional pulsed corona discharge," J. Electrostatics, Vol. 65, pp. 445-451, 2007.

[33] A. F. Nagy and J. P. Fournier, "Calculated zenith intensity of the second positive band of molecular nitrogen," J. Geophysical Research, Vol. 70, pp. 5981-5981, 1965.

[34] M. Simek, V. Babicky, M. Clupek, S. DeBenedictis, G. Dilecce, and P. Sunka, "Excitation of N2 and NO states in a pulsed positive corona discharge in N2, N2-O2 and N2-NO mixtures," J. Phys. D-Appl. Phys., Vol. 31, pp. 2591-2602, 1998.

[35] B. M. Penetrante and S. E. Schultheis, *Non-Thermal Plasma Techniques for Pollution Control: Part B: Electron Beam and Electrical Discharge Processing*: Springer Berlin Heidelberg, 2013.

[36] K. V. Kozlov and H.-E. Wagner, "Progress in Spectroscopic Diagnostics of Barrier Discharges," Plasma Phys., Vol. 47, pp. 26-33, 2007.
[37] K. Shimizu and T. Oda, "Emission spectrometry for discharge plasma diagnosis," Sci. Technology of Advanced Materials, Vol. 2, pp. 577-585, 2001.
[38] K. Teranishi, N. Shimomura, S. Suzuki, and H. Itoh, "Development of dielectric barrier discharge-type ozone generator constructed with piezoelectric transformers: effect of dielectric electrode materials on ozone generation," Plasma sources Sci. Technology, Vol. 18, pp. 045011, 2009.
[39] T. Namihira, S. Tsukamoto, D. Wang, H. Hori, S. Katsuki, R. Hackam, *et al.*, "Influence of gas flow rate and reactor length on NO removal using pulsed power," IEEE Trans. Plasma Sci., Vol. 29, pp. 592-598, 2001.
[40] P. Talebizadeh, H. Rahimzadeh, M. Babaie, S. J. Anaghizi, H. Ghomi, G. Ahmadi, *et al.*, "Evaluation of residence time on nitrogen oxides removal in non-thermal plasma reactor," PloS one, vol. 10, p. e0140897, 2015.
[41] I. Nagao, M. Nishida, K. Yukimura, S. Kambara, and T. Maruyama, "NOx removal using nitrogen gas activated by dielectric barrier discharge at atmospheric pressure," Vacuum, Vol. 65, pp. 481–487, 2002.
[42] M. Okubo, T. Miyashita, T. Kuroki, S. Miwa, and T. Yamamoto, "Regeneration of diesel particulate filter using nonthermal plasma without catalyst," IEEE Trans. Industry Appl., Vol. 40, pp. 1451-1458, 2004.
[43] M. Okubo, T. Miyashita, T. Kuroki, S. Miwa, and T. Yamamoto, "Regeneration of diesel particulate filter using nonthermal plasma without catalyst," 37th Industry Appl. Conf., Annual Meeting. pp. 1833-1840, 2002.
[44] T. Nomura, Y. Ehara, T. Ito, and M. Matsuyama, "Effect of applied voltage frequency on NOx removal rate for a superimposing discharge reactor," J. Electrostatics, Vol. 49, pp. 83-93, 2000.

Pouyan Talebizadeh received the B.Sc. and M.Sc. degrees from Shahid Bahonar University of Kerman in 2008 and 2011, and his Ph.D. degree from Amirkabir University of Technology in 2016 in mechanical engineering. He is an assistant professor of mechanical Engineering Department, Graduate University of advanced Technology, Kerman, Iran. His current research interests include two phase flow, environmental pollution control, emission reduction, Non-thermal plasma technology, HVAC systems, optimization, and numerical modeling.

Hassan Rahimzadeh received the B.Sc. and M.Sc. degrees in mechanical engineering from the West Virginia Institute of Technology, Montgomery, WV, USA, and West Virginia State University, Morgantown, WV, USA, and the Ph.D. degree in instrumentation measurement from New South Wales University, Sydney, Australia, in 1977, 1978, and 1986, respectively. He has been with the Department of Mechanical Engineering, Amirkabir University of Technology, Tehran, Iran. His current research interests include two phase flow (physical and numerical modeling), non-themral plasma technology, hydraulics structures, environmental pollution control, renewable energy, and instrumentation.

Saeed Javadi Anaghizi received the B.S. degree in Physics from the Shahrood University of Technology, Shahrud, Iran in 2010, and the M.S.degree in photonics from the Laser and Plasma Institute, Shahid Beheshti University, Tehran, Iran in 2013. He is currently employed in central laboratory of the Shahid Beheshti University as a Scanning Electron Microscope technical assistant. His current research interests include gas dis-charges plasmas, biofuels emission reduction, environmental pollution control, thin film coating technology, Surface analysis and non-thermal plasma and its Application in industry and science.

Hamid Ghomi was born in Iran 1972 and he has received the B.S. degree in applied physics in 1995 and MSc in atomic physics in 1998 and Ph.D. degree in 2004 from Shahid Beheshti University Tehran, Iran. Since 2004 he has been the faculty member of Laser and Plasma Research Institute of Shahid Beheshti University. His current research interest is Gas discharges and surface interaction with plasma, Plasma interaction with bio samples, Nano particle syntheses by discharges.

Meisam Babaie received his B.S. degree in fluid mechanical engineering from Shahrood University of Technology and M.S. degree in energy systems engineering from K. N. Toosi University of Technology in 2005 and 2008, respectively. He received his Ph.D. in the school of Chemistry, Physics and Mechanical Engineering at Queensland University of Technology, Brisbane, Australia. He is currently a lecturer at Petroleum and Gas Engineering Division, School of Computing, Science and Engineering (CSE), University of Salford, Manchester, United Kingdom. His main research interests include emission treatment, plasma science, liquefied natural gas, petroleum economics and simulation.

Richard Brown received his BE (Hons) in Mechanical Engineering from the University of Technology Sydney, his BTh from the Sydney College of Divinity and his PhD degree in combustion from the University of Sydney in 1984, 1986 and 1996, respectively. He completed postdocs at the CSIRO Division of Atmospheric Research and at the Toyohashi University of Technology before joining the academic staff of the Queensland University of Technology in 2000. He is an Associate Professor whose main research interests are thermodynamics and fluid mechanics with a focus on renewable energy and emissions.